TRAJECTORY OPTIMIZATION USING DISCRETE SETS OF PSEUDOIMPULSES: A REVIEW OF ADVANTAGES AND DIFFICULTIES

Yuri Ulybyshev
Rocket-Space Corporation ENERGIA, Korolev, Moscow Region, 141070, Russia,
+7-903-595-3885; yuri.ulybyshev@rsce.ru, yuri.ulybyshev@gmail.com

Abstract: *A feature review of new methods for continuous thrust spacecraft trajectory optimization is presented. The methods are based on a trajectory discretization by small segments and on a near-uniform discrete approximation of thrust directions by a set of pseudoimpulses with an inequality constraint for each segment. The optimization problem formulation is to minimize the total characteristic velocity with terminal conditions. The optimal impulse in each segment can be presented by the sum of non-zero pseudoimpulses with a constraint on the total characteristic velocities of the pseudoimpulses. The terminal conditions are presented as a linear matrix equation. A matrix inequality on the sums of the pseudo-impulses is used to transform the problem into a large-scale linear programming form. The continuous burns include a number of adjacent segments and a post-processing of the linear programming solutions is needed to form a sequence of the burns. An optimal number of the burns is automatically determined. The methods provide flexible opportunities for the trajectory computation in complex missions with various requirements and constraints. Summary of various application examples is presented. Advantages and difficulties of the methods are discussed.*

Keywords: *Spacecraft Trajectory Optimization, Linear Programming Application, Interior-point methods, Review.*

1. Introduction

The optimization problem of continuous thrust spacecraft trajectories has been studied extensively [1-12]. The optimization methods for the trajectories have been mainly of two types: indirect and direct techniques or their combinations. Indirect methods attempt to solve the two-point boundary-value problem based on the Pontryagin's maximum principle [13]. In the boundary value problem, the unknown costate variables are very sensitive and difficult to guess. Direct methods convert the problem into parameter optimization, which is in turn solved using, as a rule, non-linear programming methods [12, 14]. The methods are attractive because explicit consideration of the necessary optimal conditions is not required. A general review of space trajectory optimization methods was presented by Betts [15].

Linear programming represents one of the well-known optimization methods successfully used to solve many complex application problems in engineering, economics, and operations research. But classical linear programming has not been practically used for the optimization of continuous thrust trajectories. Ulybyshev and Sokolov [6] have developed a method for optimization of many-revolution, low-thrust maneuvers in the vicinity of the geostationary orbit. The method uses pseudo-maneuvers with either positive or negative transverse directions for every trajectory segment (half a revolution) so that it is possible to state the problem in terms of classical linear programming with a number of decision variables equal to quadruple the number of the revolutions in the orbit transfer.

In the 1990s, linear programming underwent a revolution with the development of polynomial-time algorithms known as interior-point methods [16] that perform more effectively than the classical simplex methods. This makes it possible to develop effective methods that use large-scale linear programming for spacecraft trajectory optimization.
The new methods are based on two ideas. The first is a well-known discretization of time, in the general case, on non-uniform segments. The second is the key idea, based on a near-uniform discrete approximation of a control space (i.e. thrust direction and magnitude) by a set of pseudo-impulses with an inequality constraint for each segment.
The paper is presented a review of author's previous works [17-26] in which the key idea was used for optimization of more trajectory types and a discussion for advantages and difficulties of the methods. The paper contains three major parts. The first is a presentation of the basic method. The second is a systematic mathematical representation of constrained trajectory optimization problem. Third is a review of major qualitative and computational features for various application examples and a discussion.

2. Trajectory optimization based on discrete sets of pseudoimpulses

2.1. Basic method for unconstrained problems

We consider a point-mass spacecraft with a limited thrust. The equations of the spacecraft motion can be expressed as

$$\frac{d\mathbf{Y}}{dt} = \mathbf{f}[\mathbf{Y}, P(t), \mathbf{e}(t), t], \tag{1}$$

where $\mathbf{Y}^{\mathbf{T}}(t) = [\mathbf{r}^{\mathbf{T}}(t),\ \mathbf{V}^{\mathbf{T}}(t), M(t)]$ is state vector; $\mathbf{r}$ is radius vector; $\mathbf{V}$ is spacecraft velocity vector ; $M(t)$ is spacecraft mass; t is time. The controls are defined as the thrust direction $\mathbf{e}$ and the thrust $P(t)$. The optimal control problem formulation considered here is to minimize a performance index that is the total characteristic velocity.

Terminal conditions for the trajectory are $\mathbf{F}[\mathbf{Y}(t_f)] = \mathbf{P}_f$, where $\mathbf{F}$ is a vector function of a state vector at the final time t_f; $\mathbf{P}_f$ is an m-dimension specified vector of the terminal conditions.
Introduce a set of segments as the partition $[t_0, t_1, t_2, \ldots, t_n]$, with $t_0=0$ and $t_n=t_f$. The mesh points t_i are referred to as nodes, the intervals $\Delta t_i=[t_{i+1}, t_i]$ are referred to as trajectory segments. Suppose that approximate values of the state vectors at the nodes $\mathbf{Y}(t_i)$ are known, then for the constant controls at each segment, we can write

$$\mathbf{P_f}(t_f) = \mathbf{P_f^*}(t_f) + \sum_{i=1}^{n} \frac{\partial \mathbf{F}(t_i)}{\partial \mathbf{V}} \cdot \Delta V_i \mathbf{e}_i\ , \tag{2}$$

where $\mathbf{P}_f^*$ is a vector of the terminal parameters computed along a trajectory without any maneuvers, $\partial \mathbf{F}(t_i)/\partial \mathbf{V}$ is a matrix of partial derivatives; $0 \le \Delta V_i \le \Delta V_{\max}$ is characteristic velocity for i-th segment.
The simplest case of the control space for the thrust vector is a plane. We consider an i-th segment independent of all the other segments. Suppose that the thrust direction in the plane is arbitrary. Without loss of generality, let a dimensionless characteristics velocity or impulse for

the segment be $\Delta V_i \leq 1$. All of the possible thrust directions can be present as a set of pseudo-impulses $\mathbf{e}_i^{(j)}$ within the unit circle with a small angle of $\Delta\varphi = 2\pi/k$ between them (Fig. 1a). Suppose that there is an optimal impulse $\Delta\mathbf{V}_{i\text{opt}}$ for the i-th segment.

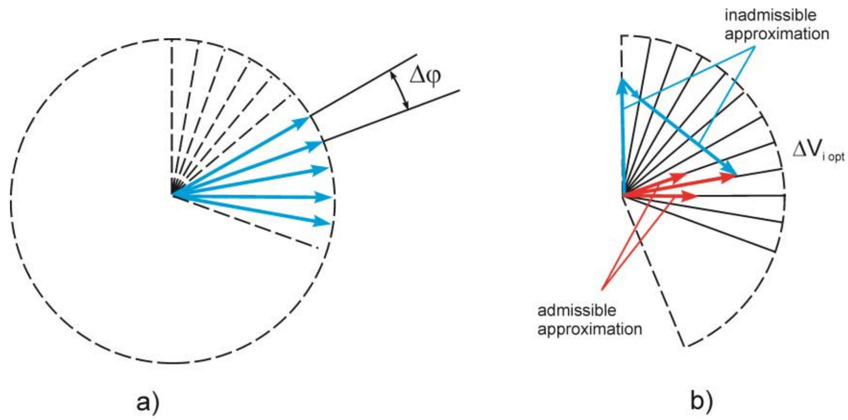

Figure 1. Set of pseudo-impulses in a plane

Thus we can present the optimal impulse by the sum

$$\Delta\mathbf{V}_{i\,\text{opt}} = \sum_1^k \Delta V_i^{(j)} \mathbf{e}_i^{(j)} \tag{3}$$

with a constraint for the characteristic velocities of the pseudo-impulses (Fig. 1b):

$$\sum_1^k \Delta V_i^{(j)} \leq 1 \tag{4}$$

The optimal impulse approximation by the pseudo-impulses is a sum of the two nearest neighbor pseudo-impulses. In a similar way, we consider a three-dimensional case for the possible thrust directions (see Fig. 2).

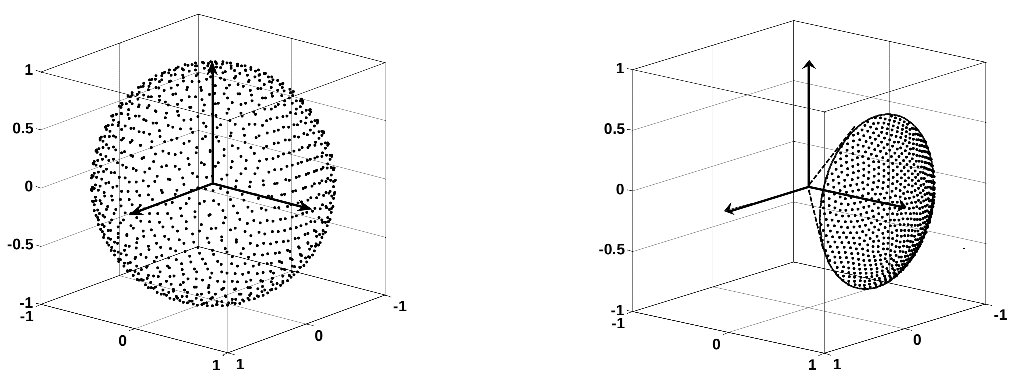

a) **b)**

Figure 2. Near uniform point distributions in 3D space

Define a $(n\times k)$-dimension vector of nonnegative decision variables

$$\mathbf{X}^{\mathrm{T}} = [\Delta V_1^{(1)}, \Delta V_1^{(2)}, .. \Delta V_1^{(k)}, \Delta V_2^{(1)}, \Delta V_2^{(2)}, .. \Delta V_2^{(k)}, .. \Delta V_n^{(k)}] \tag{5}$$

For the vector, the following linear inequality can be written

$$\mathbf{AX} \leq \mathbf{b}\ , \tag{6}$$

where $\mathbf{A}$ is a $n\times(n\times k)$-dimension matrix of the following form (all of the unspecified elements equal to zero)

$$\mathbf{A} = \left.\underbrace{\begin{bmatrix} \underbrace{111...1}_{\mathrm{k}} & & & \\ & \underbrace{111...1}_{\mathrm{k}} & & \\ & & .... & \\ & & & \underbrace{111...1}_{\mathrm{k}} \end{bmatrix}}_{\mathrm{n\times k}}\right\} \mathrm{n} \tag{7}$$

and a n-dimension vector $\mathbf{b}^{\mathbf{T}} = \left[1,\ 1,\ 1.....1,\ 1\right]$.

The terminal conditions from Eq. (2) can be expressed as

$$\Delta \mathbf{P}_f = \mathbf{P}_f - \mathbf{P}_f^* = \mathbf{A_e X}, \tag{8}$$

where $\Delta \mathbf{P}_f$ is a target vector, $\mathbf{A_e}$ is a $m\times(n\times k)$-dimension matrix of partial derivatives

$$\mathbf{A_e} = \begin{bmatrix} \underbrace{\frac{\partial F_1}{\partial V_1^{(1)}} \quad \frac{\partial F_1}{\partial V_1^{(2)}} \quad ... \quad \frac{\partial F_1}{\partial V_1^{(k)}}}_{k} & \underbrace{\frac{\partial F_1}{\partial V_2^{(1)}} \quad \frac{\partial F_1}{\partial V_2^{(2)}} \quad .... \quad \frac{\partial F_1}{\partial V_1^{(k)}}}_{k} & .... & \underbrace{\frac{\partial F_1}{\partial V_n^{(1)}} \quad \frac{\partial F_1}{\partial V_n^{(2)}} \quad .... \quad \frac{\partial F_1}{\partial V_n^{(k)}}}_{k} \\ \underbrace{\frac{\partial F_2}{\partial V_1^{(1)}} \quad \frac{\partial F_1}{\partial V_1^{(2)}} \quad .... \quad \frac{\partial F_2}{\partial V_1^{(k)}}}_{k} & \underbrace{\frac{\partial F_2}{\partial V_2^{(1)}} \quad \frac{\partial F_2}{\partial V_2^{(2)}} \quad .... \quad \frac{\partial F_2}{\partial V_2^{(k)}}}_{k} & .... & \underbrace{\frac{\partial F_2}{\partial V_n^{(1)}} \quad \frac{\partial F_2}{\partial V_n^{(2)}} \quad .... \quad \frac{\partial F_2}{\partial V_n^{(k)}}}_{k} \\ ..... & .... & ... & .... \\ \underbrace{\frac{\partial F_m}{\partial V_1^{(1)}} \quad \frac{\partial F_m}{\partial V_1^{(2)}} \quad .... \quad \frac{\partial F_m}{\partial V_1^{(k)}}}_{k} & \underbrace{\frac{\partial F_m}{\partial V_2^{(1)}} \quad \frac{\partial F_m}{\partial V_2^{(2)}} \quad .... \quad \frac{\partial F_m}{\partial V_2^{(k)}}}_{k} & ... & \underbrace{\frac{\partial F_m}{\partial V_n^{(1)}} \quad \frac{\partial F_m}{\partial V_n^{(2)}} \quad .... \quad \frac{\partial F_m}{\partial V_1^{(k)}}}_{k} \end{bmatrix} \tag{9}$$

where $\partial F_q \big/ \partial V_i^{(j)}$ is a partial derivative which can be computed using analytical relations or numerically.

Introduce a $(n\times k)$-dimension vector of weight coefficients as $\mathbf{q}^{\mathbf{T}}=[1\ \ 1...1\ \ 1]$ for the equal segments . Then, a performance index corresponding to the minimum characteristic velocity of the transfer can be written as

$$J = \min\left(\mathbf{q}^{\mathbf{T}} \cdot \mathbf{X}\right) \tag{10}$$

As the result, we have a classical linear programming problem with constraints of a linear inequality and equality given by Eqs. (9) and (11), respectively. The elements of the decision variable vector **X** must be nonnegative and constrained

$$0 \le \Delta V_i^{(j)} \le 1. \tag{11}$$

The presented linear programming form is a large-scale problem but modern scientific software, such as the MATLAB®[27], contains effective algorithms for sparse matrix computations including large-scale linear programming.

2.2. Post-processing

The segments are formally considered independent of each other. Therefore, an additional post-processing and validation for the linear programming solutions are required (see Fig. 3). It is necessary to find all of the segments corresponding to the non-zero decision variables. The adjacent segments among these should be joined in burns. If two (or three in a three-dimensional case) decision variables belong to a segment then the thrust magnitude and direction should be computed from the vector sum of the corresponding pseudo-impulses. It should be noted that the optimal number of the burns is automatically determined in the post-processing.

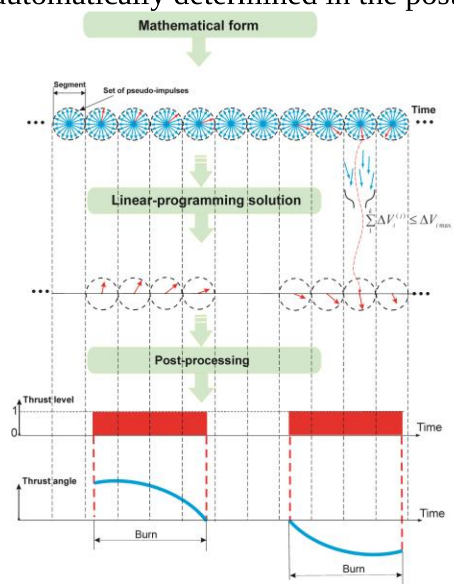

Figure 3. Post-processing of the linear programming solutions

3. Optimization of Constrained Trajectories

3.1. Typical constraints for spacecraft trajectories

The real space missions are often required to satisfy not only terminal conditions but also some specific requirements. As examples, there are constraints for interior-points in the form of boundary conditions and/or inequalities, constraints and/or preferences for some thrust directions, burn intervals, use of a multi-mode propulsion system with a combination of high-, medium-, and/or low-thrust, and other operational constraints. It is significant that the methods provide flexible opportunities for computation and design of optimal trajectories with various requirements and constraints. For such complex missions, an extension and/or modification of the basic linear programming form is required (i.e. transformation of the matrices $\mathbf{A}$, $\mathbf{A_e}$, the weight vector $\mathbf{q}$, the set of segments, and/or sets of pseudo-impulses). A schematic diagram in Fig. 4 illustrates the transformations for most used requirements and constraints.

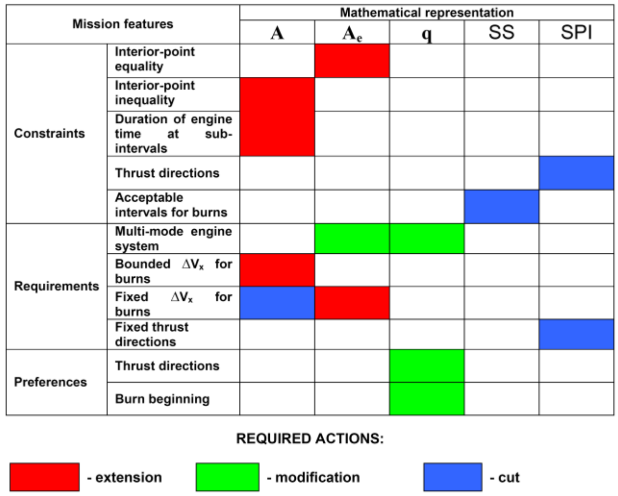

Figure 4. Constraint representations (SS – set of segments; SPI – set of pseudo-impulses).

3.2. Interior-point equality constraints

Each l-dimension interior-point equality constraint of $\mathbf{F}_{IP}[Y(t_{f\ IP})] = \mathbf{P}_{IP}$ needs additional rows in the matrix $\mathbf{A_e}$

$$\mathbf{A_e} = \begin{bmatrix} & & \mathbf{A_e'} & & & \\ \frac{\partial \mathbf{F}_{IP}}{\partial V_1^{(1)}} & \frac{\partial \mathbf{F}_{IP}}{\partial V_1^{(2)}} & \ldots.. & \frac{\partial \mathbf{F}_{IP}}{\partial V_\tau^{(k-1)}} & \frac{\partial \mathbf{F}_{IP}}{\partial V_\tau^{(k)}} & \mathbf{O}_{l\,\mathrm{x}\,[(n\text{-}1)\,\mathrm{x}\,k]} \end{bmatrix}, \tag{12}$$

where $\mathbf{A_e'}$ is the matrix in Eq.(9), $\mathbf{O}_{l\,\mathrm{x}\,[(n\text{-}1)\,\mathrm{x}\,k]}$ is the zero matrix, and τ is an index of the last segment preceding the instant $t_{f\,IP}$. In this case, the matrix $\mathbf{A_e}$ has a dimension of (l+m)x(nxk).

3.3. Interior-point inequality constraints

An inequality constraint related to an engine time $\Delta t_{E\max}$ at a time subinterval (as an example for spacecraft using electrojet engines) is presented as a quantity of the adjacent segments corresponding to the subinterval with an extension of the matrix $\mathbf{A}$ and vector $\mathbf{b}$ as

$$\mathbf{A} = \begin{bmatrix} & & & \mathbf{A'} & & \\ \mathbf{O}_{1\times[(l-1)\times k]} & \underbrace{\Delta t_{l\max} \quad \ldots. \quad \Delta t_{l\max}}_{k} & \ldots. & \underbrace{\Delta t_{s\max} \quad \ldots. \quad \Delta t_{s\max}}_{k} & \mathbf{O}_{1\times[(n-s)\times k]} \end{bmatrix} \tag{13a}$$

$$\mathbf{b^T} = [1,\ 1,\ 1\ldots..1,\ 1, \Delta t_{E\max}], \tag{13b}$$

where $\mathbf{A'}$ is the base matrix as in Eq.(7), $\mathbf{O}_{1\times[(l-1)\times k]}$ and $\mathbf{O}_{1\times[(n-s)\times k]}$ are zero string vectors. General interior-point inequality constraints are

$$Q[\mathbf{Y}(t)] \le 0 \quad \text{for } 0 \le t_b \le t \le t_e \le t_f \,, \tag{14}$$

where t_b and t_e are the begin and end times of a constrained trajectory part. The problem must be treated as a sequence of constrained segments. Suppose that s is the first segment for that $t_b \le t_s$ and $s+m$ is the last segment for that $t_{s+m} \le t_{e,}$. In addition to Eq.(6), we have the following m-inequalities:

$$Q(t_l) = Q^*(t_l) + \sum_{i=1}^{i=l} \sum_{j=1}^{k} \partial Q \big/ \partial V_i^{(j)} \cdot \Delta V_i^{(j)} \le 0 \,, \tag{15}$$

where $s \le l \le s+m$ is the segment index for the interval between t_b and t_e , $Q^*(t_l)$ is the function (14) computed along free trajectory, and $\partial Q \big/ \partial V_i^{(j)}$ is a partial derivative. Therefore the matrix **A** (7) with a dimension of $(n+m)\text{x}(n+k)$ can be expressed as (all of the unspecified elements equal to zero):

$$\mathbf{A} = \begin{bmatrix}
111...1 & & & & & & & & & \\
 & 111...1 & & & & & & & & \\
 & & ..... & & & & & & & \\
 & & & 111...1 & & & & & & \\
 & & & & 111...1 & & & & & \\
 & & & & & .... & & & & \\
 & & & & & & 111...1 & & & \\
 & & & & & & & 111...1 & & \\
 & & & & & & & & .... & \\
 & & & & & & & & & 111...1 \\
\mathbf{A}_{n+1,1} & \mathbf{A}_{n+1,2} & .... & \mathbf{A}_{n+1,s} & & & & & & \\
\mathbf{A}_{n+2,1} & \mathbf{A}_{n+2,2} & .... & \mathbf{A}_{n+2,s} & \mathbf{A}_{n+2,s+1} & & & & & \\
.... & .... & .... & .... & .... & .... & & & & \\
\mathbf{A}_{n+m,1} & \mathbf{A}_{n+m,2} & ..... & \mathbf{A}_{n+m,s} & .\mathbf{A}_{n+m,s+1} & .... & \mathbf{A}_{n+m,s+m} & & &
\end{bmatrix} \tag{16}$$

where

$$\mathbf{A}_{n+l,i} = \left[\partial Q \big/ V_i^{(1)} \quad \partial Q \big/ V_i^{(2)} \quad .... \quad \partial Q \big/ V_i^{(k)} \right] \tag{17}$$

is a k-dimension row vector of partial derivatives. The $(n+m)$-dimension vector **b** is:

$$\mathbf{b}^{\mathbf{T}} = [1 \quad 1 \qquad .... \quad 1 \quad -Q^*(t_s) \quad -Q^*(t_{s+1}) \quad .... \quad -Q^*(t_{s+m})] \tag{18}$$

Thrust direction constraints can be considered in an explicit form through corresponding sets of pseudo-impulses. Preferences for the thrust directions and/or modes of the propulsion system are presented in an explicit form through the weight vector **q**.

4. Advantages of pseudoimpulse set methods

4.1. Summary of examples for optimal spacecraft trajectories

Major qualitative and computational features of various application examples [17-26] are presented in the Table 1.

Table 1. Summary of application examples

№	Trajectory type	t_f	Solution type	Partial derivatives model	Mass model	Const-raints	Segment	Thrust directions, k	Number of n	Number of Decision variables	Number of Non zero variables	Number of Burns	Ref.
1	HEO station-keeping	30 days	Linear	Near elliptical orbit	Constant	T	Arc of 10° in true anomaly	In plane, 36	1080	38,880	~900	~60	[17]
2	LT non-coplanar transfer from GTO to GEO	29 days	Non-linear, iterative	Inverse-square gravity field	Constant		One burn	In plane, 360	80	28,280	46	46	[17]
3	MT non-coplanar transfer	8.6 hours	Non-linear, iterative	Inverse-square gravity field	Constant		Arc of 10° in argument of latitude	3D, 1000	72	72,000	1713	3	[17]
4	LT rendezvous with flyby	30 rev.	Linear	Near circular orbit	Constant	IPE	150 s	In plane, 61	1080	65,880	515	60	[18]
5	Non-coplanar launch to Moon orbit	560 s	Linear, iterative	Uniform gravity	Variable	TD, T	4 s	3D in hemisphere 2799	140	391,860	~140	2	[19]
6	Proximity maneuvers	2 rev.	Linear	Near circular orbit	Constant	IPE, IPI	40 s	In plane, 360	288	103,680	4-100	4-72	[23]
7	Collision avoidance maneuvers	2 rev.	Linear, iterative	Near circular orbit	Constant	IPI	40 s	3D, 1000	288	288,000	~200	3	[23]
8	Moon landing with constraints	400 s	Linear, iterative	Uniform gravity	Variable	IPI, TD	2.5 s	In plane	160	57,600	~100	2-4	[20]

9	Rendezvous for different thrust-to-weight ratios	2 days	Linear	Near circular orbit	Constant		2.5 min	3D, 500	1080	540,000	~60-1080	1-60	[22]
10	Earth-to-Mars transfer	193 days	Non-linear, iterative	Helio-centric inverse-square gravity field	Constant		~2 days	In plane, 360	100	36,000	100	1	[21]
11	Non-coplanar LT transfers to GEO with constraints	17 days	Non-linear, iterative	Inverse-square gravity field	Variable	Eclipse, T	Arc of 10° in true anomaly	3D, 180	1800	16,200	~1000	~100	[24]
12	Non-coplanar LT transfers to HEO	7 days	Non-linear, iterative	Inverse-square gravity field	Variable		Arc of 10° in true anomaly	3D, 180	1800	16,200	~400	~50	[24]
13	EML2 Halo-orbit stationkeeping	1 year	Non-linear, iterative	Numeric for reference orbit with full ephemeris model	Constant	IPI	~1.6 hours	3D, 1000	100 for each half revo lution	100,000	~1000	1-2 for each half revo lution	[25, 26]

The abbreviations in the table are: HEO – High Elliptical Orbit; GEO – GEostationary Orbit; GTO – Geo-Transfer Orbit; EML2 – Earth-Moon Libration Point L_2; LT, and MT – Low-, and Medium-Thrust, respectively; T - constraints on engine time at time subintervals; IPE - Interior-Point Equality constraints; IPI – Interior-Point Inequality constraints; TD - Thrust Direction constraints; and 3D – three dimensional space.

4.2. Optimal number of maneuvers

A very complex astrodynamics problem is determination of optimal maneuver number [2, 12, 28-32]. To the present day, the problem for a general case remains unsolved. There are solutions for simple particular cases. As an example, it is unconstrained optimal trajectories in uniform gravity field [28]. The next example is linear impulsive rendezvous trajectories for near-circular orbits [12]. For more cases, the optimal number of maneuvers is specified or bounded [31]. Some methods using the Lawden's primer vector theory [28] makes possible to verify optimality of an *N*-impulse trajectory and to perfect the trajectory through transformation to an *N*+1 impulse solution [30]. Prussing derives an upper bound on the number of impulses required for a linear optimal solution [31]. He also marked [32, page 204] that "However, for a nonlinear system no upper bound exists." As is well-known from the Lawden's primer vector theory [28], nonsingular optimal space trajectories must be formed by intervals of the maximum thrust and coast arcs separated by a finite number of switches, and the optimal thrust direction is always aligned along the primer vector. For trajectories with a bounded thrust and an unknown number of the burns, an iterative method with updating a switch function can be used [12, Chap. 3.7].

For the pseudoimpulse set methods, the mentioned property of nonsingular trajectories is mean that the characteristic velocity for the segments of a burn must correspond to ΔV_{imax}. The exceptions are only the first and last segments in the burn. A non-compliance with these qualitative properties for optimal unconstrained trajectories may indicate that it is a singular solution. For an inverse-square gravity field, the primer vector is a function of the eccentric anomaly with periodic and secular terms [28]. Therefore the angular thrust direction rate in the burn must be of the same order as the orbital angular velocity, and a high-frequency chattering should be lacking. To our knowledge, for a general bounded thrust orbit transfer case, determination of the optimal number of burns is an unsolved problem. We believe that in the new methods the automatically determined in the post-processing number of burns is optimal. Our computational experience shows that if a linear programming solution satisfying the boundary conditions exists then the post-processing solution does not collide with the cited qualitative properties of the optimal space trajectory theory. A strict proof that the number of the burns is optimal is difficult. The pseudoimpulse set methods in opposite other methods can be automatically determined the optimal number of maneuvers.

More complex case for a maneuver optimal number determination is the trajectories with interior-point constraints. As an illustrative example of the problem, optimal lunar landing trajectories that is modeled by a variable-mass point moving over a flat surface with a uniform gravity field [20] (#8 in Table 1) can be presented. Optimal thrust profiles are presented for unconstrained trajectory in Fig. 5a and constrained trajectory in Fig. 5b. Each segment is depicted as a color-filled rectangle with a height equal to a thrust level. The colors of the rectangles correspond to the required pitch angles in compliance with the shading scale (the right side in the figure). According to the Lawden's primer vector theory [28], the optimal unconstrained trajectory consists of two burns (Fig. 5a). The second trajectory is included interior-point constraints: constant thrust angle of -90° at the landing terminal phase, a transition phase with bounds for maximum thrust angle, and a safety profile with the free fall time no less than t_{AB}=40 s. The last constraint is related to contingency situations so that the spacecraft should be able to abort the descent process at any time with a free fall time no less than the

safety time t_{AB} , that is needed for performing operations in a contingency aborting of the landing [20]. In fact, it is a four-burn trajectory.
Perhaps, the automatic determination of the maneuver optimal number is a major advantage of the methods.

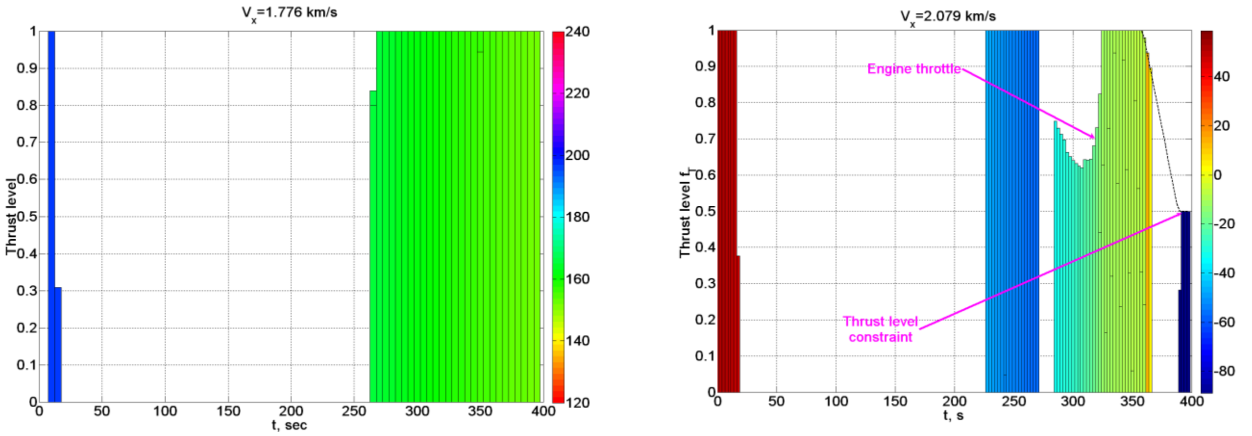

a) b)

Figure 5. Thrust profiles for Moon landing

4.3. Iterative solutions and nonlinear problems

In a sense, spacecraft trajectories can be divided into two categories: a motion near to a reference trajectory and a general case with substantial changes of initial trajectory parameters and respectively the partial derivatives. For the first (often named as a stationkeeping problem), the partial derivatives in Eq. (9) even for nonlinear cases are known with a relatively high-precision. They can be computed analytically or numerically. Analytical derivative computation was used for stationkeeping of HEO (#1 in Table 1)[17]. The numerical partial derivatives based on full-ephemeris model can be used for an EML2 Halo-orbit stationkeeping (#13 in Table 1) [25, 26]. A corresponding example of long-term simulation for the halo-orbit using high-fidelity ephemeris model that incorporates the effects of lunar eccentricity, solar gravity, and solar radiation pressure (JPL DE421 ephemeris) is depicted in Fig. 6.

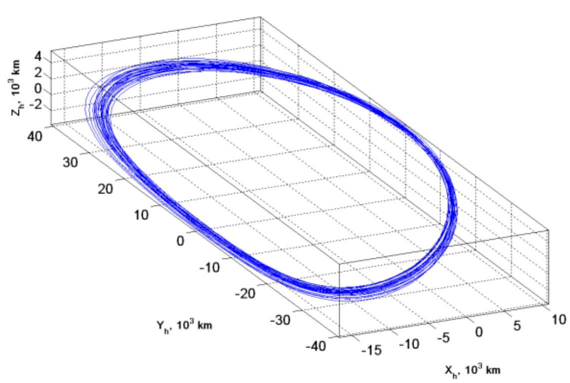

Figure 6. One year controlled evolution of halo-orbit

For the general case, an intermediate trajectory and, respectively, the partial derivatives in Eq. (9), are usually not known a priori. For such cases, an iterative technique with a refinement of the partial derivatives at each iteration can be used. For the first iteration, we define an initial guess for intermediate trajectory parameters. The unknown parameters have, as a rule and often, monotonic variations and/or known variation ranges between the initial and terminal parameters. As an example, it can be a variation of the semimajor axis between initial and terminal values (with the exception of bi-elliptic transfers). Based on the linear programming solution, the parameters are refined for the second iteration, etc. to satisfy the specified terminal conditions. As a result, the solution is found as a sequence of trajectories generated by controls on corresponding iterations. Notice a substantial distinction of the methods from known methods of successive approximations, for an example, the sequential linearization method [14] where in the process of iterations, there is a descent in the control space takes place: on every iteration the variations (more exactly additions) to the control law are determined from the previous iteration. In the suggested method a reference trajectory satisfying a preset control is found, and a new control law is determined at each iteration. In essence one can say that there is a descent in the space of reference trajectories occurs here. For the general case, a convergence of such processes requires special studies, but there are examples that illustrate the convergence to a single solution for different initial approximations.

An example of iterative process convergences for a low thrust orbital transfer between a circular orbit (semimajor axis of 17000 km and inclination of 28.5°) and GEO (semimajor axis of 42164 km and zero inclination) is presented in Fig. 7 [24]. For the transfer is assumed t_f = 50 orbits (~18 days), the initial thrust acceleration of $4.4 \cdot 10^{-6}$ km/s^2, and the specific thrust of 2500 s. The following variants of the initial guess for the semimajor axis $a(t)$ approximation (dashed blue lines) are used: constant initial orbit (Fig. 7a); constant final orbit (Fig. 7b); linear variation between the initial and final values (Fig. 7c), and variation of $a(t)$ under for the constant thrust acceleration equivalent to a coplanar trajectory (i.e. transfer between the initial and final orbits without changes in the orbit inclination, Fig. 7d). All of the types of the initial approximations ensured convergence to one and the same solution (bold red lines). For each iteration, the functions are depicted by thin black lines.

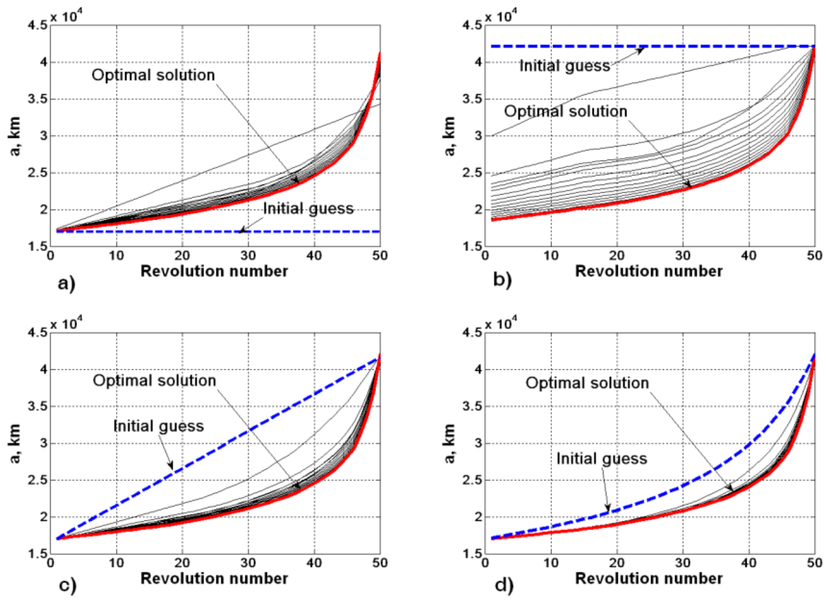

Figure 7. Solution convergence for different initial guess

The absence of a solution with a low-thrust means, most likely, that the thrust acceleration (i.e. the spacecraft thrust-to-weight ratio) is small for the trajectory or the problem formulation with the terminal conditions and constraints is degenerate. For the last case, an attempt of the solution for a very high-thrust acceleration can be used as a validation test of the possible degeneracy.
Contrary to the methods presented here, the optimal control techniques in the form of an iterative solution for a two-point boundary value problem for the state and adjoint variables are difficult to apply. The main difficulty with these methods is getting started, i.e., finding a first estimation of the unspecified conditions for the state and adjoint variables [33]. Moreover, the adjoint variables do not have a physical meaning, and thus, it can be difficult to find a reasonable initial guess for them [33].

4.4. Trajectory optimization with interior-point constraints

In section 4.2 was mentioned the example of the lunar landing trajectory with a safety descent profile (Fig. 8b). The descent profile (altitude versus vertical velocity) - $h(V_h)$ for unconstrained trajectory and lower bound of the safety profile are presented in Fig. 8a. The safety profile constraint is required for a sequence of adjacent segments (between a segment immediately preceding to the first violation of the constraint and up to $t=t_f-t_{AB}$=360 s, t_f=400 s), the corresponding inequalities should be met (see Sect. 3.3)[20].

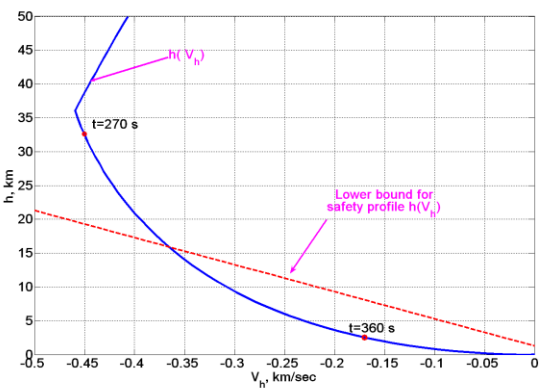

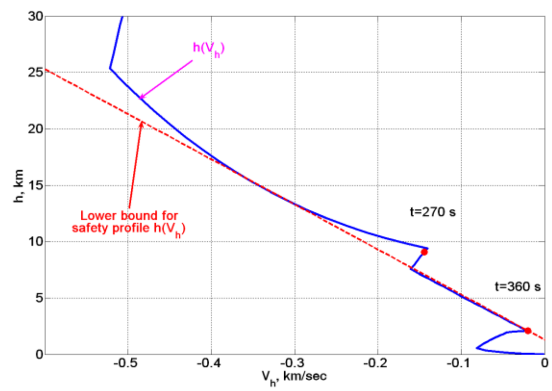

. **a) unconstrained profile** **b) constrained profile**

Figure 8. Descending profile for Moon landing

The next example is optimization of a spatial collision avoidance for a relative motion trajectory with a minimum allowable range and return to the initial trajectory [23] (#7 in Table 1). The trajectory must be pass at tangent to a sphere with radius of the range. Therefore it is needs to find the tangent point (or points) based on an iterative approach with interior-point inequalities. The optimal relative motion trajectory is depicted in Fig. 9 (red line). The thrust directions for the segments are depicted by blue arrows. For a comparison, the initial collision trajectory (green line) is also presented. The trajectory parts with the constraint violations are displayed as bold green arcs. The optimal trajectory is includes three continuous maneuvers.

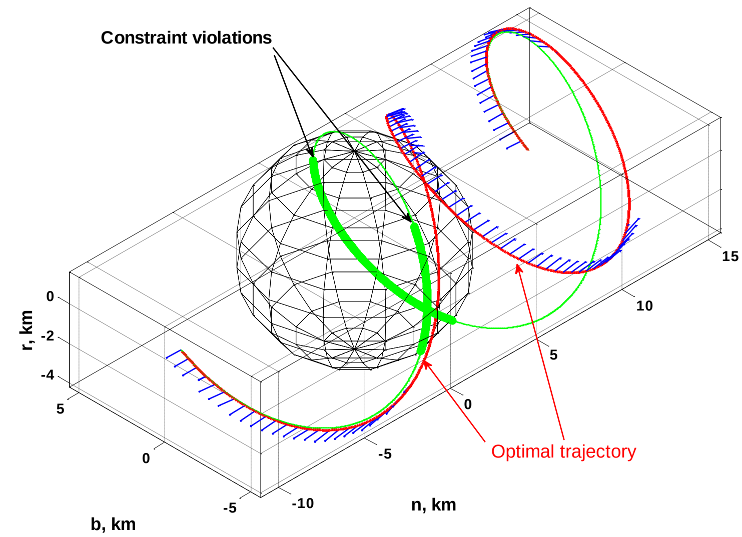

Figure 9. Collision avoidance trajectory

There is a nonstandard illustrative example with cyclic constraints (the burn durations no more than 3 hours and the time between them no less than 3 hours) for the low thrust orbital transfer between circular orbit and GEO in previous section (#11 in Table 1)[24]. The constraints can be related with electric power balance. The burn distribution is presented in Fig. 10 (72 segments for each revolution at 50 revolutions interval). Each segment with the non-zero thrust is depicted as a gray-filled rectangle. The colors of the rectangles correspond to the required yaw angle magnitudes (the pitch angles near to zero) in compliance with the shading scale (the right side in the figure).

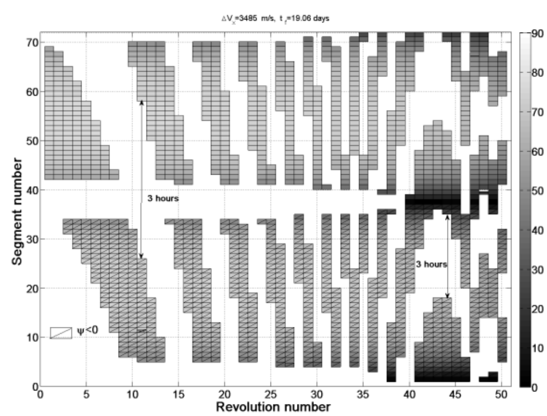

Figure 10. Burn distribution for cyclic constraints

4.5. Influence of thrust-to-weight ratio on optimal trajectories

A major spacecraft design parameter is the thrust-to-weight ratio that have a significant influence on the optimal solutions. In the mission design, it is very important estimations of energy losses and maneuver possibilities with a reduced thrust-to-weight ratio (as an example, for contingency situations). The solution of such problems is difficult and required special algorithms.

As examples, two-day (30 revolutions) rendezvous trajectories are considered (#9 in Table 1)[22]. The trajectories are close to mission profiles for the rendezvous of a spacecraft to the International Space Station. For impulsive solutions (i.e. for the high thrust), there is a range of initial phase angles (the geocentric angle between the spacecraft and space station) for that required characteristic velocity ΔV_x for the trajectories is almost equal and near to the optimal orbit transfer between the orbits. Similar solutions are exist for bounded thrusts. The optimal phase range depends substantially on the thrust-to-weight ratio. The required ΔV_x as functions of the phase angles for different values of the thrust acceleration are shown in Fig. 11. For comparison, the phase range for the optimal impulsive solutions is also depicted (dashed red line).

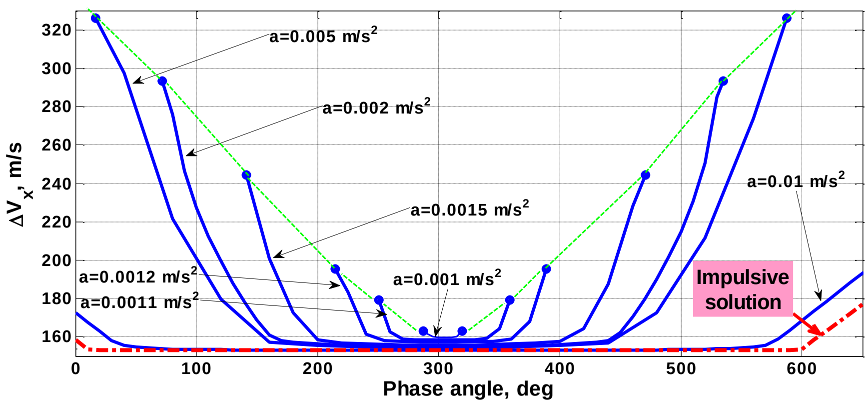

Figure 11. Required ΔV_x for different thrust accelerations

There is a minimum thrust acceleration for that the solution of the rendezvous problem with the specified boundary conditions and final time exists. The solution is corresponded to the continuous thrust at the transfer time interval, i.e. it is one multi-revolution burn with continuous change of the thrust direction. There are different trajectory types: near to impulsive (medium thrust); two burns at an quantity of adjacent revolutions (medium and low thrust); two burns at all of the revolutions (low thrust); near to continuous multi-revolution burns (very low thrust). An example of the last type solution (phase angle is ~520°) is presented in Fig. 12, where the burn distribution is given as sequences of adjacent segments for each revolution. Each segment is depicted as a color-filled rectangle. The colors correspond to the required thrust yaw angles (the pitch angles near to zero) in compliance with the color axis scaling (the right side of the figure).

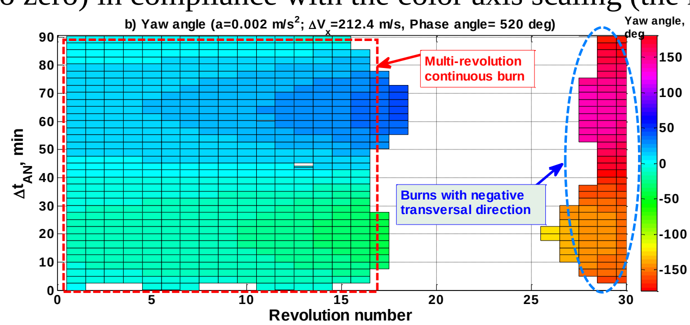

Figure 12. Example of burn distribution and thrust direction

Continuous solution changes for the range of the possible phase angles are shown in Fig. 13. The solutions with the limit phase angles are corresponded to the continuous thrust for the transfer time interval, i.e. it is one multi-revolution burn but with one switching of the yaw angle.

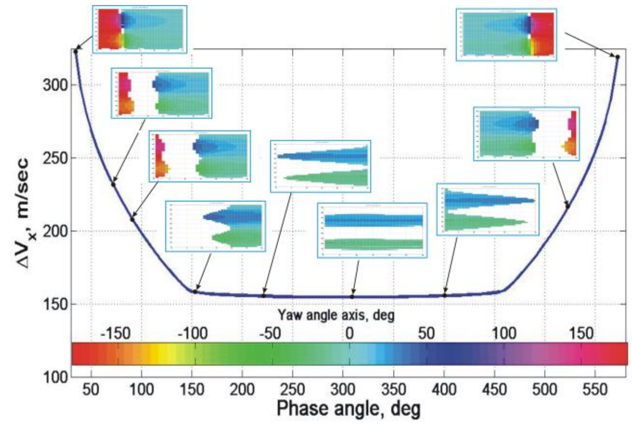

Figure 13. Changes of solutions in range of possible phase angles.

The thrust-to-weight ratio and the phase angle are defined not only the required ΔV_x but the general solution structure as well. A set of solution structures is depicted in Fig. 14

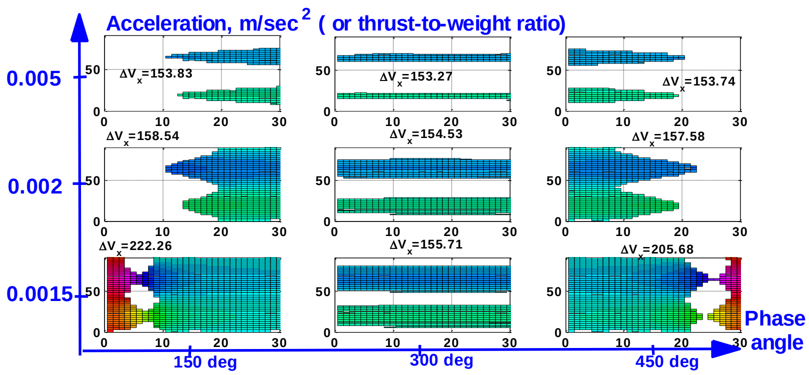

Figure 14. Changes of solutions for different phase angles and thrust-to-weight ratios

The last example is the station-keeping of halo orbits in the vicinity of the EML2 (#13 in Table 1)[25,26]. Solutions with different thrust at the first half-revolution for the halo-orbit, are presented in Fig. 15. The black arrows depict thrust directions at the corresponding segments. The last trajectory is an almost continuous maneuver for the full half-revolution. The twenty-fold decrease of the thrust acceleration requires more than a two-fold increase of the characteristic velocity (ΔV_x=23.43 m/s for a_p=1×10^{-6} km/s^2, and ΔV_x=54.52 m/s for a_p=0.05×10^{-6} km/s^2).

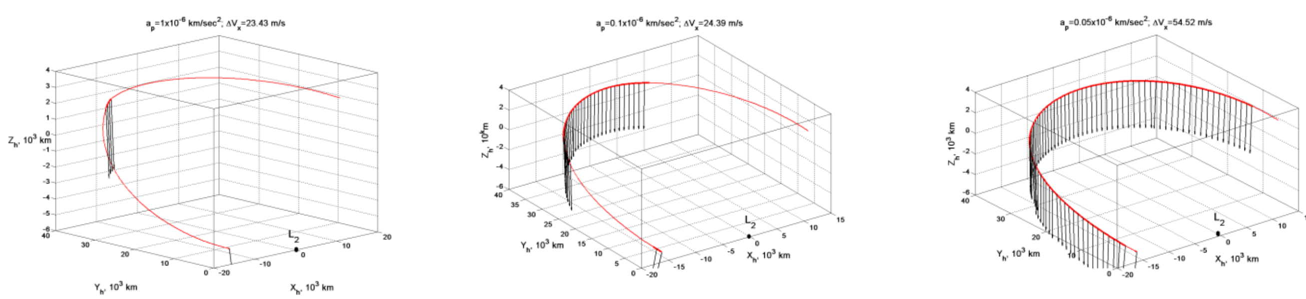

a) **b)** **c)**

Figure 15. Trajectory and maneuvers for different thrust-to-weight ratios

4.6. General optimal control problem

The concept of the discrete pseudo-impulse sets can be extended to a more general optimal control problem [21]. The approach is also based on discretization of the system motion on small segments and a discrete approximation of the control space by a set of pseudo-control vectors for each segment.

5. Some difficulties of pseudoimpulse set methods

5.1. Large scale

The methods are transformed the spacecraft trajectory optimization problem to large-scale problems that required a special software. As an example, for the rendezvous problem (#9 in Table 1)[22] with 1080 segments and 500 pseudo-impulses in each segment, the number of the decision variables is (1080 segments x 500 pseudo-impulses)=540,000. The matrix **A** has the dimension of 1080×540000. But it is a sparse matrix with a low number of the non-zero elements (for the example, it is ~0.1%). Modern scientific software, such as the MATLAB®, have effective algorithms for sparse matrix computations [27] including the large-scale linear programming.

5.2. Free terminal time

The describable methods are used a specified terminal time in an explicit form (direct t_f) or implicit form (as an example, a final revolution number). The solution problems for free terminal time (including the minimum-time problems) required special techniques in form of a sequence of the solutions with decreasing final times t_f .

5.3 Solution convergence difficulties

All of the iterative methods for spacecraft trajectory optimization can be present convergence difficulties (non convergence, slow convergence, etc.). These difficulties should be considered for each specific optimization problem. There is not a general technique. Some techniques are presented in textbooks [14, 33]. With regard to the pseudoimpulse set methods, it can also be a more detailed analysis of the segment duration and pseudoimpulse set discretization. In a sense, the methods are correspond to an implicit form of the well-known Euler method for integration of ordinary differential equations. Therefore, a suitable value of the integration step for the Euler method can be recommended as an initial value for the segment durations.

6. Conclusion

A review of new spacecraft trajectory optimization methods is presented. The methods are based on a discretization of the trajectory on small segments and the key idea is a discrete approximation for the space of the possible thrust directions by a set of pseudo-impulses for each segment. On the one hand it greatly increased the number of the decision variables, but it also permitted a transformation of the problem to a classical linear programming form. The methods provide an effective possibility for the trajectory optimization with various operational constraints such as interior-point boundary conditions and/or inequalities, thrust level, thrust directions, etc. The methods may also be used as a part of the spacecraft design for an analysis of the consistency for constraints and determination of a required thrust-to-weight ratio for a mission type. Advantages and difficulties of the methods are discussed based on numerous application examples.

7. References

[1] Melton, R. G., Lajoie, K. M., and Woodburn, J. W., "Optimum burn scheduling for low-thrust orbital transfers," Journal of Guidance, Control, and Dynamics, Vol. 12, No.1, 1989, pp.13-18.

[2] Enright, P.J., and Conway, B.A., "Discrete Approximations to Optimal Trajectories Using Direct Transcription and Nonlinear Programming, "Journal of Guidance, Control, and Dynamics, Vol. 15, No. 4, 1992, pp. 994-1002.

[3] Seywald, H., "Trajectory Optimization Based on Differential Inclusion," Journal of Guidance, Control, and Dynamics, Vol. 17, No. 3, 1994, pp. 480-487.

[4] Kluever, C.A., " Low-Thrust Orbit Transfer Guidance Using an Inverse Dynamics Approach," Journal of Guidance, Control, and Dynamics, Vol. 18, No.1,1995, pp. 187-189.

[5] Kechichian , J.A., "Reformulation of Edelbaum's Low-Thrust Transfer Problem Using Optimal Control Theory," Journal of Guidance, Control, and Dynamics , Vol. 20, No.5, 1997, pp.988-994.

[6] Ulybyshev, Y.P., and Sokolov, A.V., "Many-Revolution, Low-Thrust Maneuvers in Vicinity of Geostationary Orbit," Journal of Computer and System Sciences International, Vol. 38, No. 2, 1999, pp. 255-261.

[7] Herman, A.L., and Spencer, D.B., "Optimal, Low-Thrust Earth-Orbit Transfers Using Higher-Order Collocation Methods," Journal of Guidance, Control, and Dynamics, Vol. 25, No. 1, 2002, pp. 40-47.

[8] Fahroo, F., and Ross, I. M.," Direct Trajectory Optimization by a Chebyshev Pseudospectral Method," Journal of Guidance, Control, and Dynamics, Vol. 25, No. 1, 2002, pp. 160-167.

[9] Haberkorn, T., Martinon, P., and Gergaud, J., " Low Thrust Minimum-Fuel Orbital Transfer: A Homotopic Approach," Journal of Guidance, Control, and Dynamics, Vol. 27, No. 6, 2004, pp. 1046-1060.

[10] Ranieri, C.L. and Ocampo, C.A., "Optimization of Roundtrip, Time-Constrained, Finite Burn Trajectories via an Indirect Method," Journal of Guidance, Control, and Dynamics, Vol.28, No. 2, 2005, pp.306-314.

[11] Ross, I.M., Gong, Q., and Sekhavat P., "Low-Thrust, High-Accuracy Trajectory Optimization," Journal of Guidance, Control, and Dynamics, Vol. 30, No.4, 2007, pp. 921-933.

[12] *Spacecraft Trajectory Optimization*, Ed.by B. A. Conway, Cambridge University Press, 2010.

[13] Pontryagin, L.S., Boltyanskii, V.G., Gamkrelidze, R.V., and Mishchenko, E.F., *The Mathematical Theory of Optimal Processes*, Wiley, 1962, Chap.2.

[14] Betts, J., *Practical Methods for Optimal Control and Estimation Using Nonlinear Programming*, Second Edition, SIAM, 2009.

[15] Betts, J., "Survey of Numerical Methods for Trajectory Optimization," Journal of Guidance, Control, Dynamics, Vol. 21, No. 2, 1998, pp. 193-207.

[16] Wright, M.H., “The Interior-Point Revolution in Optimization: History, Recent Developments, and Lasting Consequences,” Bulletin of the American Mathematical Society, Vol. 42, No. 1, 2004, pp. 39–56.
[17] Ulybyshev Y., “Continuous Thrust Orbit Transfer Optimization Using Large-Scale Linear Programming,” Journal of Guidance, Control, and Dynamics, Vol. 30, No. 2, 2007, pp.427-436.
[18] Ulybyshev Y , “Optimization of Multi-Mode Rendezvous Trajectories with Constraints”, Cosmic Research, Vol. 46, No. 2, 2008, pp. 133-147.
[19] Ulybyshev Y , “Concept of pseudo-impulses for spacecraft trajectory optimization,” Polyot (Flight), No. 2, 2008, pp.52-60 (in Russian).
[20] Ulybyshev Y., “Spacecraft Trajectory Optimization Based on Discrete Sets of Pseudo-Impulses, ” Journal of Guidance, Control, and Dynamics, Vol. 32, No.4, 2009, pp.1200-1217.
[21] Ulybyshev Y., “Discrete Pseudocontrol Sets for Optimal Control Problems,” Journal of Guidance, Control, and Dynamics, Vol.33, No.4, 2010, pp.1133-1142.
[22] Ulybyshev, Y., “Optimal Rendezvous Trajectories as a Function of Thrust-to-Weight Ratio,” AIAA Astrodynamics Specialist Conference, Toronto, Ontario, AIAA Paper 2010-7663 , 2010, 15 pp..
[23] Ulybyshev, Y., “Trajectory Optimization for Spacecraft Proximity Operations with Constraints,” AIAA Guidance, Navigation, and Control Conference, Portland, OR, AIAA Paper 2011-7663, 2011, 15 pp..
[24] Ulybyshev, Y., “Optimization of Low Thrust Orbit Transfers with Constraints,” Cosmic Research, Vol. 50, No. 5, 2012, pp. 403-418.
[25] Ulybyshev Y., “Stationkeeping Strategy and Possible Lunar Halo Orbits for Long-Term Space Station,” AIAA Guidance, Navigation, and Control Conference, National Harbor, MR, AIAA Paper 2014-0274, 2014, 15 pp.
[26] Ulybyshev Y., “Long-Term Stationkeeping of Space Station in Lunar Halo Orbits,” Journal of Guidance, Control, and Dynamics, Vol. 38, No. 6, 2015, pp. 1063-1070.
[27] *MATLAB® Users Guide*, The Math Works, Inc., Natick, MA, 2003, Chap. 16.
[28] Lawden, D.F., *Optimal Trajectories for Space Navigation*, Batterworths, London, 1963.
[29] Edelbaum T.N., “How many impulses?,” Astronautics and Aeronautics, Vol. 5, Nov. 1967, pp. 64-69.
[30] Lion P. M. and Handelsman M., "Primer vector on fixed-time impulsive trajectories." AIAA Journal, Vol. 6, No. 1, 1968, pp. 127-132.
[31] Prussing J.E., “Optimal Impulsive Linear Systems: Sufficient Conditions and Maximum Number of Impulses,” Journal of the Astronautical Sciences, Vol. 43, No. 2, 1995, pp. 195–206.
[32] Longuski J.M., Guzman J.J., and Prussing J.E., *Optimal Control with Aerospace Applications*, Springer, New York, 2014.
[33] Bryson, A. E. Jr., and Ho, Y.-C., *Applied Optimal Control*, Hemisphere, New York, 1975.